CHEMISTRY OF MATERIALS

ARTICLE

pubs.acs.org/cm

Di(4-methylphenyl)methano-C_{60} Bis-Adduct for Efficient and Stable Organic Photovoltaics with Enhanced Open-Circuit Voltage

Yen-Ju Cheng,* Ming-Hung Liao, Chih-Yu Chang, Wei-Shun Kao, Cheng-En Wu, and Chain-Shu Hsu*

Department of Applied Chemistry, National Chiao Tung University 1001 Ta Hsueh Road, Hsin-Chu, 30010 Taiwan, Republic of China

Supporting Information

ABSTRACT: A new class of fullerene bis-adducts—di(4-methylphenyl)methano-C_{60} bis-adduct (**DMPCBA**), di(4-fluorophenyl)methano-C_{60} bis-adduct (**DFPCBA**), and diphenylmethano-C_{60} bis-adduct (**DPCBA**)—were rationally designed and easily synthesized. Compared to the lowest unoccupied molecular orbital (LUMO) energy level of **$PC_{61}BM$** (−3.95 eV), the double functionalization effectively raises the LUMO energy levels of these fullerene materials to ca. −3.85 eV, regardless of the substituent groups (CH_3−, F−, and H−) at the *para*-position of the phenyl rings. This phenomenon suggests that the plane of the phenyl groups is preferentially parallel to the fullerene surface, leading to poor orbital interactions with C_{60} and negligible electronic effect. Importantly, such geometry sterically protects and shields the core C_{60} structure from severe intermolecular aggregation, rendering it intrinsically soluble, morphologically amorphous, and thermally stable. The device based on the P3HT:**DMPCBA** blend exhibited an open-circuit voltage (V_{oc}) of 0.87 V, a short-circuit current density (J_{sc}) of 9.05 mA/cm^2, and a fill factor (FF) of 65.5%, leading to a high power conversion efficiency (PCE) of 5.2%, which is superior to that of the P3HT:**$PC_{61}BM$**-based device. Most significantly, the amorphous nature of **DMPCBA** effectively suppresses the thermal-driven aggregation and thus stabilizes the morphology of the P3HT:**DMPCBA** blend. Consequently, the device retained 80% of its original PCE value against thermal heating at 160 °C over 20 h.

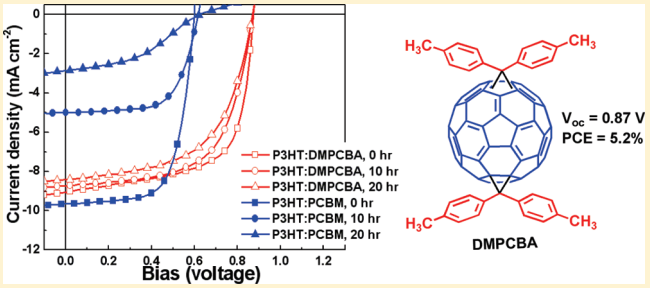

KEYWORDS: C_{60} bis-adduct, open-circuit voltage, morphological stability, organic photovoltaics

INTRODUCTION

Research on polymer solar cells (PSCs) using organic *p*-type (donor) and *n*-type (acceptor) semiconductors has attracted tremendous scientific and industrial interest in recent years.[1] A regioregular poly(3-hexylthiophene) (P3HT) and a fullerene derivative ([6,6]-phenyl-C_{61}-butyric acid methyl ester (**$PC_{61}BM$**)) are the most representative *p*-type/*n*-type material pair for polymeric bulk heterojunction (BHJ) solar cells (PSCs).[2] One of the bottlenecks for the P3HT:**$PC_{61}BM$**-based devices is the low open-circuit voltage (V_{oc}) of ca. 0.6 V, limiting power-conversion efficiencies (PCEs) to ca. 4%. It is anticipated that a PCE of up to 6% can be reasonably achieved if the V_{oc} can be significantly improved to ∼0.9 V. It has been demonstrated that the magnitude of V_{oc} value is proportional to the energy difference between the donor's highest occupied molecular orbital (HOMO) energy level and the acceptor's lowest unoccupied molecular orbital (LUMO) level.[3] At the molecular level, either lowering the HOMO level of the polymer or raising the LUMO level of the fullerene material could reach greater theoretically V_{oc} values. Although extensive research effort have been directed to the development of new low-band gap polymers by employing a donor−acceptor (D-A) approach,[4] manipulating the HOMO energy level of the D-A polymers remains challenging, because the HOMO of the polymers are not only governed by electron-rich donor units but also are associated with electron-deficient acceptor units. Besides, lowering a polymer's HOMO level may inevitably increase its optical band gap and thereby sacrifice its light-harvesting ability. Developing new fullerene-based materials that possess intrinsically high-lying LUMO energy levels is a more achievable alternative to optimize the V_{oc} value. Incorporation of electron-donating groups (EDGs) on the peripheral side of monosubstituted fullerenes has been utilized to elevate LUMO energy levels.[5] However, because of the lack of direct conjugation between the EDG and the core C_{60}, the through-space electronic effect is relatively weak. Therefore, the variations in the LUMO energy level of fullerene derivatives are too small to significantly impact the V_{oc} value. Recently, bis-adduct C_{60} derivatives have emerged as new materials with higher-lying LUMO energy levels, compared to their corresponding mono-adduct C_{60} analogues.[6] The second functionalization on the core structure of the monosubstituted C_{60} further reduces the π-conjugation and electron delocalization in the C_{60}. This structural alteration makes bis-adduct C_{60} derivatives have larger electrochemical reduction potentials and, thus, higher-lying LUMO levels. Further exploration of new class of C_{60} bis-adducts for next generation *n*-type materials is highly desirable. Another primary area of concern for traditional P3HT:**$PC_{61}BM$**

Received: June 22, 2011
Revised: July 8, 2011
Published: August 04, 2011

dx.doi.org/10.1021/cm201784w | *Chem. Mater.* 2011, 23, 4056–4062

Scheme 1. Synthesis and Chemical Structures of Diphenylmethano-Based C_{60} Bis-Adducts

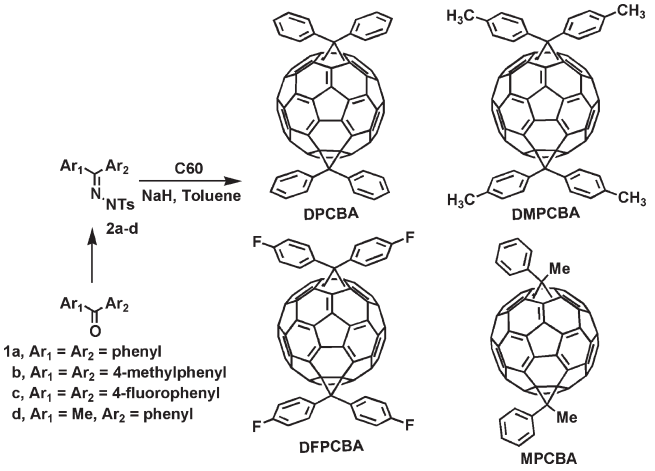

system is the morphological instability. Upon heating, spherical PCBM with high molecular mobility tends to diffuse out of the P3HT matrix and aggregate into larger clusters or single crystals.[7] Such a progressive phase segregation eventually leads to micrometer-sized D-A domains with concomitant reduction of device efficiency.

Cyclopropanation is an ideal reaction for fullerene modification, because of its high stability and small structural perturbation. Di(4-alkylphenyl)methanofullerene monoadduct derivatives have been used as *n*-type materials to blend with P3HT for PSCs. The devices have shown superior V_{oc} values, of up to 0.69 V, which is almost 100 mV higher than that of **$PC_{61}BM$**.[8] However, the short-circuit current density (J_{sc}) is relatively lower, presumably because of the higher content of insulating alkyl chains. Wudl et al. have demonstrated that the planes of the two phenyl rings in diphenylmethanofullerene prefer to lie parallel to the fullerene surface.[9] We envisaged that if a C_{60} is doubly functionalized with diphenylmethano moieties, the geometry of the two geminal diphenyl groups can sterically protect and shield the core C_{60} structure from severe intermolecular aggregation, rendering it intrinsically amorphous and highly soluble. As such, long alkyl chains on the phenyl rings to ensure solubility are not necessary. In this paper, we wish to report a new class of *n*-type materials, based on the diphenylmethano-C_{60} bis-adduct (**DPCBA**) scaffolds (see Scheme 1, presented later in this work). To investigate the electronic effect in this system, the *para* position of the four phenyl rings were substituted by weak electron-donating methyl groups and electron-withdrawing fluoro groups to afford di(4-methylphenyl)methano-C_{60} bis-adduct (**DMPCBA**), and di(4-fluorophenyl)methano-C_{60} bis-adduct (**DFPCBA**), respectively. Furthermore, methylphenylmethano-C_{60} bis-adduct (**MPCBA**) are also synthesized as a reference for comparison. A P3HT-based solar cell using **DMPCBA** as the acceptor achieved not only a high open-circuit voltage of V_{oc} = 0.87 V with an exceptional power conversion efficiency (PCE) of 5.2%, but also excellent morphological stability against thermal heating.

RESULTS AND DISCUSSION

Synthesis. The synthesis of these new materials is shown in Scheme 1. The diphenyl ketone derivatives (**1**) were first converted to the corresponding tosylhydrazone moieties (**2**). Two equivalents (2 equiv) of compound **2** were reacted with C_{60} to yield the corresponding C_{60} bis-adducts, using NaH as the base and toluene as the solvent. These C_{60} bis-adducts were separated from the corresponding monoadduct by multiple column chromatography. All the final products contain a mixture of regioisomers.

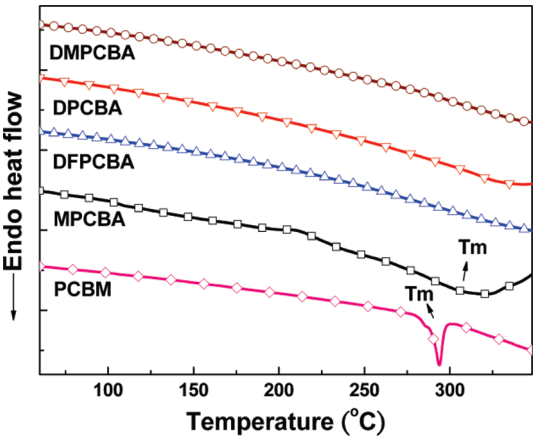

Figure 1. Differential scanning calorimetry (DSC) measurement of C_{60} bis-adducts with a heating rate of 10 °C/min.

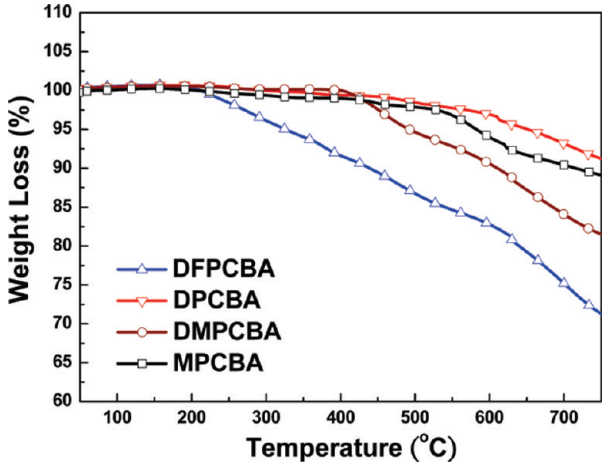

Figure 2. Thermogravimetric analysis (TGA) measurement of C_{60} bis-adducts with a heating rate of 20 °C/min.

Thermal Properties. Encouragingly, the **DPCBA**-based materials without any alkyl chain as the solublizing group exhibited excellent solubility in common organic solvents, implying that two diphenylmethano moieties on the peripheral side indeed sterically prevent spherical C_{60} from close packing. Furthermore, unlike **$PC_{61}BM$** showing a sharp melting point at 280 °C from differential scanning calorimetry (DSC) measurement, no melting thermal transition was observed for the **DPCBA**-based derivatives (see Figure 1). This again indicates that these materials are amorphous glasses that have no tendency toward thermal-driven crystallization. In contrast, by replacing a phenyl ring with a smaller methyl group, **MPCBA** shows relatively poor solubility and becomes crystalline with a melting point observed at 300 °C. In addition, these materials possess extremely high thermal stability. **DPCBA**, **MPCBA**, and **DMPCBA** showed decomposition temperature (T_d) values as high as 625, 582, and 492 °C, respectively, from the thermal gravimetric analysis

dx.doi.org/10.1021/cm201784w |*Chem. Mater.* 2011, 23, 4056–4062

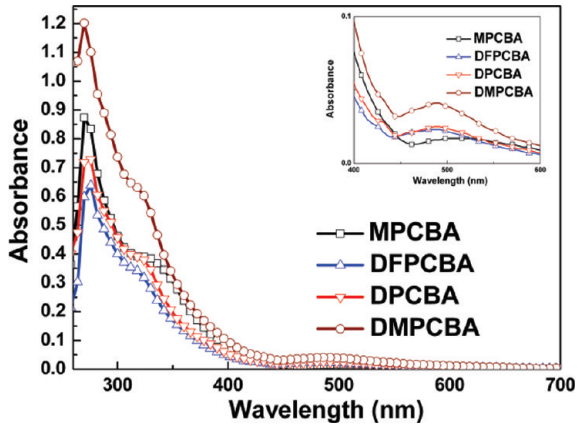

Figure 3. Absorption spectra of C_{60} bis-adducts in tetrahydrofuran (THF) solutions (10^{-5} mol/L). Inset: enlarged absorption spectra in the visible region from 400 nm to 600 nm.

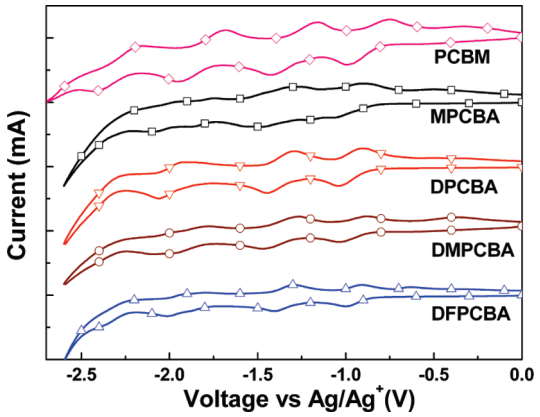

Figure 4. Cyclic voltammetry of the C_{60} bis-adducts at a scan rate of 30 mV/s.

(TGA) measurement, whereas **DFPCBA** showed the lowest T_d value, at 323 °C (see Figure 2).

Optical Properties. The absorption spectra of these materials in tetrahydrofuran (THF) solutions are shown in Figure 3. The absorption profile for each material is essentially similar. It should be mentioned that **DMPCBA** exhibited the strongest absorption intensity in the ultraviolet (UV) region, compared to the other materials under the same concentration of 10^{-5} M in THF.

Electrochemical Properties. The electrochemical properties of these materials are evaluated by cyclic voltammetry and are shown in Figure 4. In comparison to the LUMO level of **$PC_{61}BM$** monoadduct (−3.95 eV), all the bis-adduct compounds indeed showed higher LUMO energy levels. The LUMO levels of **DPCBA** and **MPCBA** were estimated to be −3.85 eV and −3.84 eV, respectively. By introducing methyl groups and fluoro groups at the *para*-positions of the phenyl groups, both the LUMO levels of **DMPCBA** and **DFPCBA** are located at −3.85 eV. These results reveal that the electronic effect on the phenyl groups is negligible and the LUMO energy levels are almost independent of the functional groups. This phenomenon has been observed in the diphenylmethaofullerene monoadduct derivatives, indicating that the phenyl groups are preferentially parallel to the fullerene surface and, thus, have poor orbital interactions with C_{60}.[7]

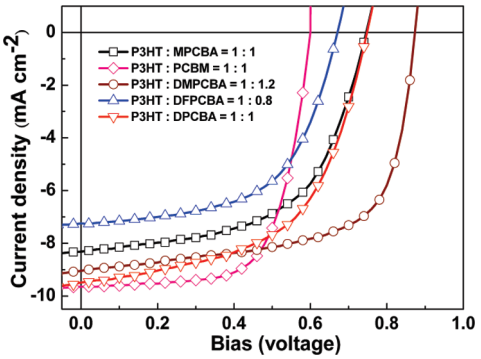

Figure 5. Current density−voltage characteristics of ITO/PEDOT:PSS/P3HT:C_{60} bis-adduct/Ca/Al devices under illumination of AM 1.5 G, 100 mW/cm^2.

Photovoltaic and Electron-mobility Characteristics. To evaluate these C_{60} bis-adducts, bulk heterojunction solar cells based on the ITO/PEDOT:PSS/P3HT:C_{60} bis-adduct/Ca/Al configuration were fabricated and characterized under simulated 100 mW cm^{-2} AM 1.5 G illumination. The current density−voltage curves of the devices are shown in Figure 5, and the corresponding device characteristics with the optimal blending ratio are shown in Table 1.

Indeed, the newly developed C_{60} bis-adducts effectively improve the V_{oc} of the devices. Compared to the performance of P3HT:**$PC_{61}BM$** (1:1, w/w)-based device, the device using P3HT:**DPCBA** blend (1:1, w/w) showed a higher V_{oc} of 0.75 V and comparable J_{sc} of 9.48 mA/cm^2, leading to a higher PCE of 4.0%. When P3HT was blended with **DFPCBA** functionalized with fluoro groups (1:0.8, w/w), the device showed a reduced V_{oc} value of 0.68 V and a J_{sc} value of 7.25 mA/cm^2 and a decreased PCE value of 2.8%. In contrast, with introducing methyl groups on the phenyl rings in **DMPCBA**, the device using P3HT:**DMPCBA** blend (1:1.2, w/w) exhibited a much-enhanced V_{oc} value of 0.87 V, a J_{sc} value of 9.05 mA/cm^2, and a higher FF value of 65.5%, yielding an impressively high PCE value of 5.2%. To the best of our knowledge, the V_{oc} value of 0.87 V is the highest value ever reported among the P3HT:fullerenoid PSCs. Furthermore, the device based on P3HT:**MPCBA** (1:1, w/w) showed a J_{sc} value of 8.32 mA/cm^2, a V_{oc} value of 0.73 V, a FF value of 57.4%, and, thus, a lower PCE of 3.5%. Note that, although the C_{60} bis-adducts contain a mixture of isomers, the devices incorporating **DMPCBA** synthesized from different batches all showed consistent and reproducible device characteristics.

The surface morphology of the blends was investigated using atomic force microscopy (AFM) phase images (Figure 6). It is found that the P3HT:**DMPCBA** thin film exhibited the most homogeneous mixing between two photoactive materials, whereas the P3HT:**MPCBA** blend showed relatively larger phase domains. The structural modification with smaller methyl groups in **MPCBA** may strengthen the intermolecular interaction between **MPCBA** molecules, leading to a more unfavorable morphology of the active layer. This comparison manifests that the diphenylmethano moiety is indeed a superior addend for C_{60} double functionalization.

To evaluate the electron mobility in the BHJ active layer via the space-charge-limited current (SCLC) method, electron-only devices (ITO/Al/P3HT:C_{60} bis-adduct/Ca/Al) were fabricated. Despite the amorphous nature, the **DPCBA** derivatives without insulating aliphatic chain showed good electron-transporting

Table 1. Device Characteristics

	weight ratio[a]	open-circuit voltage, V_{oc} (V)	short-circuit current density, J_{sc} (mA/cm^2)	fill factor, FF (%)	power conversion efficiency, PCE (%)	electron mobility[b] (cm^2/(V s))
DPCBA	1:1	0.75	9.48	55.9	4.0	1.3×10^{-4}
DMPCBA	1:1.2	0.87	9.05	65.5	5.2	9.0×10^{-5}
DFPCBA	1:0.8	0.68	7.25	57.3	2.8	9.3×10^{-5}
MPCBA	1:1	0.73	8.32	57.4	3.5	7.7×10^{-5}
PC$_{61}$BM	1:1	0.60	9.65	67.4	3.9	1.3×10^{-4}

[a] Weight ratio of P3HT to the C_{60} bis-adducts. [b] Based on ITO/Al/P3HT:C_{60} bis-adduct/Ca/Al devices using SCLC theory.

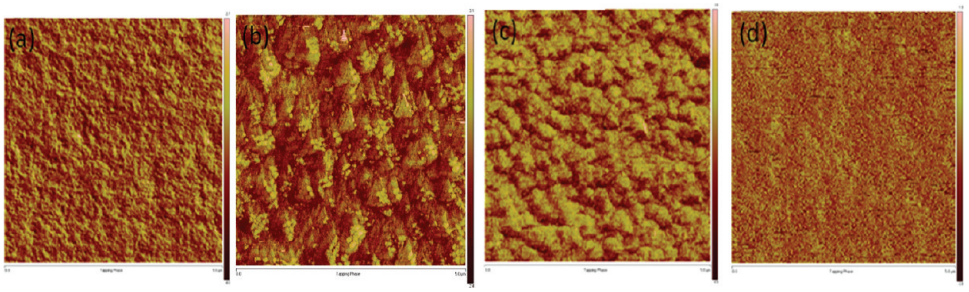

Figure 6. Atomic force microscopy (AFM) phase images of (a) P3HT:**DFPCBA** (1:0.8, w/w), (b) P3HT:**DPCBA** (1:1, w/w), (c) P3HT:**MPCBA** (1:1, w/w), and (d) P3HT:**DMPCBA** (1:1.2, w/w) films thermally annealed at 150 °C for 5 min.

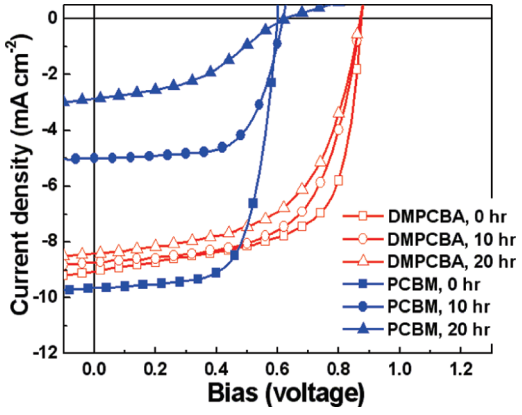

Figure 7. $J-V$ characteristics of PSCs based on the P3HT:**PC$_{61}$BM** (1:1, w/w) and P3HT:**DMPCBA** (1:1.2, w/w) blend before and after isothermal heating at 160 °C for 10 and 20 h.

properties. All the composites exhibited the electron mobilities approximately at the magnitude of 1×10^{-4} cm^2/(V s), which is comparable to that of the P3HT/**PC$_{61}$BM** blend (1.3×10^{-4} cm^2/(V s)) under the same fabrication conditions (see Table 1).

Morphological Stability against Heating. To investigate morphological stability under the influence of thermal treatment, we fabricated a series of devices, based on the configuration of ITO/PEDOT:PSS/P3HT:**DMPCBA**(1:1.2, w/w)/Al. These devices were isothermally heated at 160 °C for 10 and 20 h prior to the deposition of the top electrode. The corresponding P3HT:**PC$_{61}$BM** (1:1, w/w)-based reference devices were also fabricated to test the thermal stability. The current density versus potential ($J-V$) curves and the corresponding photovoltaic parameters (PCE, V_{oc}, J_{sc}, and FF), as a function of heating time at 160 °C, were plotted in Figures 7 and 8, respectively. The efficiency of the P3HT:**PC$_{61}$BM** reference device decreased dramatically, from 3.9% to 0.7% after 20 h of isothermal heating. In sharp contrast, the **DMPCBA**-based device exhibited much more stable device characteristics and the PCE smoothly degraded to 4.7% for 10 h then to 4.2% over 20 h of heating. Note that the high V_{oc} value of 0.87 V remains intact against 20 h of heating.

Optical microscopy (OM) was used to investigate the morphological alteration of the blends of micrometer size under the influence of heating (Figure 9). Thermal annealing of the P3HT:**PC$_{61}$BM** blend induced a severe macrographic alteration, forming needle-shaped **PC$_{61}$BM** crystals hundreds of micrometers in length.[7d] In contract, the morphology of the P3HT:**DMPCBA** (1:1.2, w/w) blend remains almost unchanged before and after the thermal annealing. The high thermal stability is associated with the amorphous nature of **DMPCBA** to preserve the device characteristics.

CONCLUSIONS

In summary, we have rationally designed and successfully synthesized a new class of diphenylmethano-based C_{60} bis-adducts without incorporating aliphatic side chains as a solubilizing group. The plane of the phenyl groups lying parallel to the fullerene surface sterically protects and shields the core C_{60} structure from severe intermolecular aggregation, rendering it intrinsically soluble, morphologically amorphous, and thermally stable. The double functionalization raises the LUMO energy level of **DMPCBA** by ~0.1 eV, compared to that of **PC$_{61}$BM**. The device based on the P3HT:**DMPCBA** blend exhibited a V_{oc} value of 0.87 V, a J_{sc} value of 9.05 mA/cm^2, and a FF value of 65.5%, leading to a high PCE of 5.2%, which is superior to that of the P3HT:**PC$_{61}$BM**-based device. To the best of our knowledge, the V_{oc} value of 0.87 V represents the highest value ever reported among the devices based on P3HT:fullerenoid materials. Most

dx.doi.org/10.1021/cm201784w |*Chem. Mater.* 2011, 23, 4056–4062

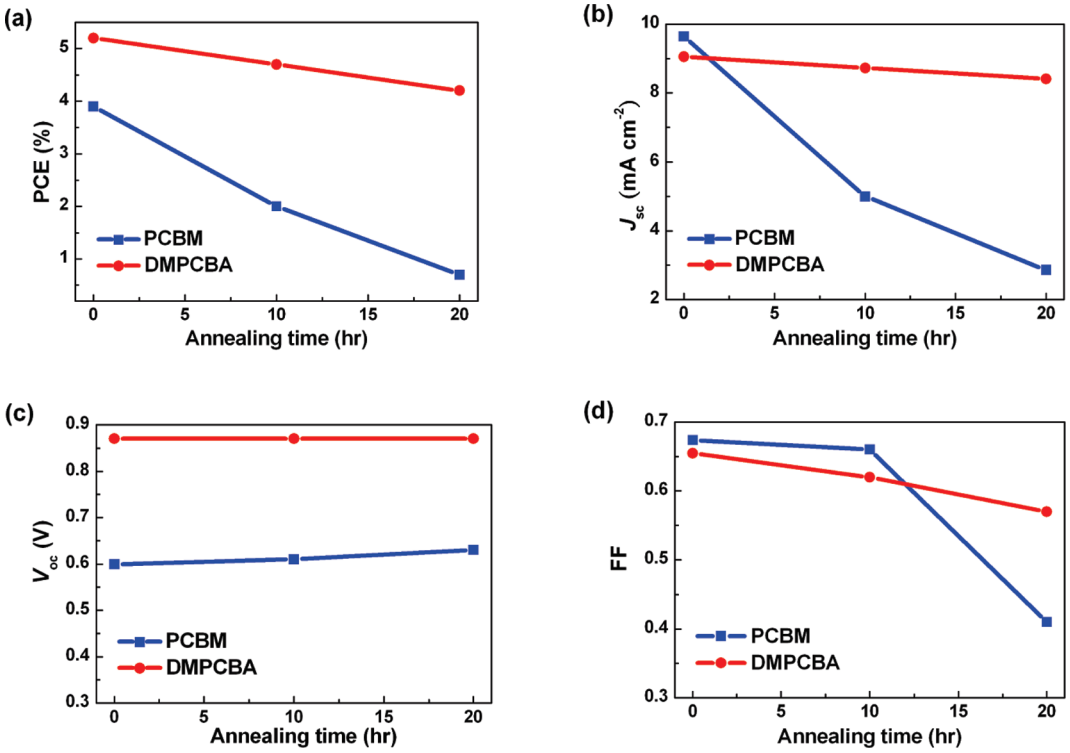

Figure 8. Photovoltaic parameters of PSCs based on the P3HT:**$PC_{61}BM$** (1:1, w/w) blend and P3HT:**DMPCBA** blend (1:1.2, w/w), as a function of heating time at 160 °C. (a) PCE, (b) J_{sc}, (c) V_{oc}, and (d) FF.

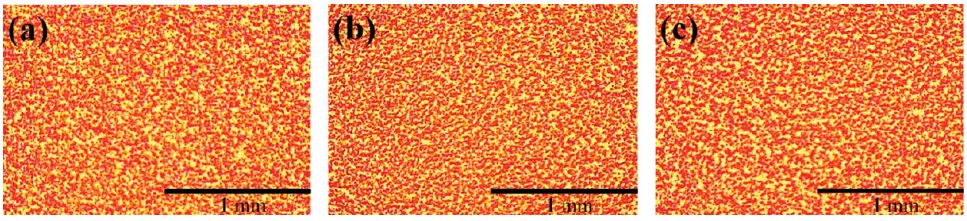

Figure 9. Optical microscopy of P3HT:**DMPCBA** (1:1.2, w/w) films after thermal annealing at 160 °C for (a) 0 h, (b) 10 h, and (c) 20 h. No obvious change is observed.

significantly, the amorphous nature of **DMPCBA** beneficially suppresses the thermal-driven crystallization and thus stabilizes the morphology of the P3HT:**DMPCBA** blend. As a result, the device retained 80% of its original PCE value against thermal heating at 160 °C over 20 h.

EXPERIMENTAL SECTION

General Measurement and Characterization. All chemicals were purchased from Aldrich and Acros, unless otherwise specified. ^{1}H were recorded on a Varian Unity-300 spectrometer. Differential scanning calorimetry (DSC) was measured on TA Q200 Instrument under a nitrogen atmosphere at a heating rate of 10 °C/min, and thermogravimetric analysis (TGA) was recorded on a Perkin−Elmer Pyris system under nitrogen atmosphere at a heating rate of 20 °C/min. Absorption spectra were collected on a Hitachi U-4100 spectrophotometer. Electrochemical cyclic voltammetry (CV) was conducted on a CH Instruments electrochemical analyzer as the workstation. A carbon glass was used as the working electrode, Pt wire was used as the counter electrode, and Ag/Ag^+ electrode (0.01 M $AgNO_3$, 0.1 M TBAP in acetonitrile) was used as the reference electrode. In a mixed solution of *o*-dichlorobenzene/acetonitrile (4:1) with 0.1 M $TBAPF_6$ (tetrabutylammonium hexafluorophosphate) at 100 mV/s. LUMO = $-e(E_{red}^{on} + 4.75)$, where E_{red}^{on} is the onset reduction potential (in volts) versus Ag/Ag^+. The AFM images under tapping mode were taken on a Veeco INNOVA Microscope AFM system with a INNOVA Nanodrive controller. The optical microscopy images were measured by Zeiss Axiophot.

Device Fabrication and Characterization. The ITO/glass substrates were first cleaned in ultrasonic baths of isopropyl alcohol, acetone, and isopropyl alcohol. After the ITO/glass substrate was dried in an oven at 80 °C for 10 min, they were treated with UV-ozone for 20 min. Then, the surface of the ITO substrate was modified by spin-coating PEDOT:PSS solution (Clevios P AI4083), followed by baking at 150 °C for 10 min in air. The mixture solution of P3HT (18 mg) and C_{60} bis-adducts with different ratios (18 mg for **$PC_{61}BM$**, **DPCBA**, and **MPCBA**; 21.6 mg for **DMPCBA**; 14.4 mg for **DFPCBA**) in 1 mL of *o*-dichlorobenzene (ODCB) was then spin-coated onto the PEDOT:PSS layer. The P3HT:C_{60} bis-adduct blend film was then put into glass petri dishes while still wet, to undergo a solvent annealing process. After drying, the samples were annealed at 140 °C for 10 min. The thermal

dx.doi.org/10.1021/cm201784w |*Chem. Mater.* 2011, 23, 4056–4062

stability of the P3HT:$PC_{61}BM$- and P3HT:**DMPCBA**-based devices were subjected to sustained heating at 150 °C for various times prior to the cathode electrode deposition. The cathode, which was made of calcium (10 nm thick) and aluminum (100 nm thick), was sequentially evaporated through a shadow mask under high vacuum ($<10^{-6}$ Torr). Each sample consists of four independent pixels defined by an active area of 0.04 cm^2. Finally, the devices were encapsulated and characterized in air. The devices were characterized under 100 mW/cm^2 AM 1.5 simulated light measurement (Yamashita Denso solar simulator). Current density ($J-V$) characteristics of PSC devices were obtained by a Keithley Model 2400 SMU system. Solar illumination conforming the JIS Class AAA was provided by a SAN-EI 300W solar simulator equipped with an AM 1.5G filter. The light intensity was calibrated with a Hamamatsu S1336-5BK silicon photodiode. The performances presented here are the average of the four pixels of each device. In order to investigate the electron mobilities of the different blend films, unipolar devices have been prepared following the same procedure except that the PEDOT:PSS layer is replaced by evaporated aluminum (100 nm). The electron mobilities were calculated according to space-charge-limited current theory (SCLC). The $J-V$ curves were fitted according to the following equation:

$$J = \left(\frac{9}{8}\right)\varepsilon\mu\left(\frac{V^2}{L^3}\right)$$

where ε is the permittivity of the blend film, μ the hole mobility, and L the film thickness.

Synthesis of Compound 2a. Compound **1a** (8 g, 43.9 mmol) and *p*-toluenesulfonyl hydrazide (9.81 g, 52.7 mmol) were dissolved in a mixed solvent of methanol (100 mL) and toluene (100 mL). The resulting mixture was refluxed using a Dean−Stark apparatus for 12 h. After cooling to room temperature, the mixture was concentrated and methanol was added, then cooled to 0 °C. The precipitated compound was then collected by filtration and washed by cold methanol three times. The solid compound was dried overnight under vacuum to get compound **2a**[10] (9 g, 59%).

Synthesis of Compound 2b. In a similar manner described above, **2b**[10] was obtained from **1b** (6.3 g, 55%).

Synthesis of Compound 2c. In a similar manner described above, **2c**[10] was obtained from **1c** (5 g, 70%).

Synthesis of Compound 2d. In a similar manner described above, **2d**[11] was obtained from **1d** (6.3 g, 62%).

Synthesis of Compound DPCBA. To a toluene solution (1 L) of compound **2a** (0.97 g, 2.8 mmol) was added sodium hydride (0.2 g, 8.3 mmol) quickly under nitrogen. After the solution was stirred at room temperature for 20 min, 0.5 equiv of C60 (1 g, 1.39 mmol) was added. The resultant purple solution was heated to 70−80 °C and stirred for 10 h. Then, the solution was heated to reflux at 120 °C and stirred for 24 h. After cooling to room temperature, the solution was extracted with $NH_4Cl_{(aq)}$. The organic layer was dried over anhydrous $MgSO_4$, and the solvent was removed by concentration. Finally, the mixture was loaded into a silica gel column, using toluene and hexane (v/v, 1/4) as the eluent. The solid was reprecipitated from toluene in methanol five times. The remaining brown was filtered and washed twice with methanol and dried overnight under vacuum to get the red brown compound **DPCBA** (146 mg, 10%). MS (FAB) *m/z*: 1053.

Synthesis of Compound DMPCBA. In a similar manner described above, **DMPCBA** was obtained from **2b** (50 mg, 11%). MS (FAB) *m/z*: 1110.

Synthesis of Compound DFPCBA. In a similar manner described above, **DFPCBA** was obtained from **2c** (55 mg, 15%). MS (FAB) *m/z*: 1124.

Synthesis of Compound MPCBA. In a similar manner described above, **MPCBA** was obtained from **2d** (60 mg, 15%). MS (FAB) *m/z*: 929.

■ ASSOCIATED CONTENT

Supporting Information. ^1H NMR spectra and mass spectrometry of the new compounds. This information is available free of charge via the Internet at http://pubs.acs.org/.

■ AUTHOR INFORMATION

Corresponding Author

*E-mail: yjcheng@mail.nctu.edu.tw (Y.-J.C.), cshsu@mail.nctu.edu.tw (C.-S.H.).

■ ACKNOWLEDGMENT

This work is supported by the National Science Council and "ATP" of the National Chiao Tung University and Ministry of Education, Taiwan.

■ REFERENCES

(1) (a) Arias, A. C.; MacKenzie, J. D.; McCulloch, I.; Rivnay, J.; Salleo, A. *Chem. Rev.* **2010**, *110*, 3. (b) Yu, G.; Gao, J.; Hummelen, J. C.; Wudl, F.; Heeger, A. J. *Science* **1995**, *270*, 1789. (c) Günes, S.; Neugebauer, H.; Sariciftci, N. S. *Chem. Rev.* **2007**, *107*, 1324. (d) Thompson, B. C.; Fréchet, J. M. J. *Angew. Chem., Int. Ed.* **2008**, *47*, 58. (e) Cheng, Y.-J.; Yang, S.-H.; Hsu, C.-S. *Chem. Rev.* **2009**, *109*, 5868.

(2) (a) Ma, W.; Yang, C.; Gong, X.; Lee, K.; Heeger, A. J. *Adv. Funct. Mater.* **2005**, *15*, 1617. (b) Li, G.; Shrotriya, V.; Huang, J.; Yao, Y.; Moriarty, T.; Emery, K.; Yang, Y. *Nat. Mater.* **2005**, *4*, 864.

(3) (a) Brabec, C. J.; Cravino, A.; Meissner, D.; Sariciftci, N. S.; Fromherz, T.; Rispens, M. T.; Sanchez, L.; Hummelen, J. C. *Adv. Funct. Mater.* **2001**, *11*, 374. (b) Scharber, M. C.; Mühlbacher, D.; Koppe, M.; Denk, P.; Waldauf, C.; Heeger, A. J.; Brabec, C. J. *Adv. Mater.* **2006**, *18*, 789. (c) Koster, L. J. A.; Mihailetchi, V. D.; Blom, P. W. M. *Appl. Phys. Lett.* **2006**, *88*, 093511.

(4) (a) Zou, Y.; Najari, A.; Berrouard, P.; Beaupré, S.; Réda Aïch, B.; Tao, Y.; Leclerc, M. *J. Am. Chem. Soc.* **2010**, *132*, 5330. (b) Piliego, C.; Holcombe, T. W.; Douglas, J. D.; Woo, C. H.; Beaujuge, P. M.; Fréchet, J. M. J. *J. Am. Chem. Soc.* **2010**, *132*, 7595. (c) Li, Z.; Ding, J.; Song, N.; Lu, J.; Tao, Y. *J. Am. Chem. Soc.* **2010**, *132*, 13160. (d) Woo, C. H.; Beaujuge, P. M.; Holcombe, T. W.; Lee, O. P.; Fréchet, J. M. J. *J. Am. Chem. Soc.* **2010**, *132*, 15547. (e) Bronstein, H.; Chen, Z.; Ashraf, R. S.; Zhang, W.; Du, J.; Durrant, J. R.; Tuladhar, P. S.; Song, K.; Watkins, S. E.; Geerts, Y.; Wienk, M. M.; Janssen, R. A. J.; Anthopoulos, T.; Sirringhaus, H.; Heeney, M.; McCulloch, I. *J. Am. Chem. Soc.* **2011**, *133*, 3272. (f) Chu, T.-Y.; Lu, J.; Beaupré, S.; Zhang, Y.; Pouliot, J.-R.; Wakim, S.; Zhou, J.; Leclerc, M.; Li, Z.; Ding, J.; Tao, Y. *J. Am. Chem. Soc.* **2011**, *133*, 4250. (g) Price, S. C.; Stuart, A. C.; Yang, L.; Zhou, H.; You, W. *J. Am. Chem. Soc.* **2011**, *133*, 4625. (h) Chen, H.-Y.; Hou, J.; Zhang, S.; Liang, Y.; Yang, G.; Yang, Y.; Yu, L.; Wu, Y.; Li, G. *Nat. Photon.* **2009**, *3*, 649. (i) Hou, J.; Chen, H.-Y.; Zhang, S.; Li, G.; Yang, Y. *J. Am. Chem. Soc.* **2008**, *130*, 16144. (j) Huang, F.; Chen, K.-S.; Yip, H.-L.; Hau, S. K.; Acton, O.; Zhang, Y.; Luo, J.; Jen, A. K.-Y. *J. Am. Chem. Soc.* **2009**, *131*, 13886. (k) Qin, R.; Li, W.; Li, C.; Du, C.; Veit, C.; Schleiermacher, H.-F.; Adersson, M.; Bo, Z.; Liu, Z.; Inganas, O.; Wuerfel, U.; Zhang, F. *J. Am. Chem. Soc.* **2009**, *131*, 14612. (l) Cheng, Y.-J.; Wu, J.-S.; Shih, P.-I.; Chang, C.-Y.; Jwo, P.-C.; Kao, W.-S.; Hsu, C.-S. *Chem. Mater.* **2011**, *23*, 2361.

(5) (a) Kooistra, F. B.; Knol, J.; Kastenberg, F.; Popescu, L. M.; Verhees, W. J. H.; Kroon, J. M.; Hummelen, J. C. *Org. Lett.* **2007**, *9*, 551. (b) Zhang, Y.; Yip, H.-L.; Acton, O.; Hau, S. K.; Huang, F.; Jen, A. K. Y. *Chem. Mater.* **2009**, *21*, 2598. (c) Yang, C.; Kim, J. Y.; Cho, S.; Lee, J. K.; Heeger, A. J.; Wudl, F. *J. Am. Chem. Soc.* **2008**, *130*, 6444. (d) Backer,

S. A.; Sivula, K.; Kavulak, D. F.; Fréchet, J. M. J. *Chem. Mater.* **2007**, *19*, 2927.

(6) (a) Lenes, M.; Wetzelaer, G.-J. A. H.; Kooistra, F. B.; Veenstra, S. C.; Hummelen, J. C.; Blom, P. W. M. *Adv. Mater.* **2008**, *20*, 2116. (b) He, Y.; Chen, H.-Y.; Hou, J.; Li, Y. *J. Am. Chem. Soc.* **2010**, *132*, 1377. (c) Cheng, Y.-J.; Hsieh, C.-H.; He, Y.; Hsu, C.-S.; Li, Y. *J. Am. Chem. Soc.* **2010**, *132*, 17381. (d) Zhao, G.; He, Y.; Li, Y. *Adv. Mater.* **2010**, *22*, 4355.

(7) (a) Yang, X.; van Duren, J. K. J.; Janssen, R. A. J.; Michels, M. A. J.; Loos, J. *Macromolecules* **2004**, *37*, 2151. (b) Swinnen, A.; Haeldermans, I.; vande Ven, M.; D'Haen, J.; Vanhoyland, G.; Aresu, S.; D'Olieslaeger, M.; Manca, J. *Adv. Funct. Mater.* **2006**, *16*, 760. (c) Yang, X.; van Duren, J. K. J.; Rispens, M. T.; Hummelen, J. C.; Janssen, R. A. J.; Michels, M. A. J.; Loos, J. *Adv. Mater.* **2004**, *16*, 802. (d) Cheng, Y.-J.; Hsieh, C.-H.; Li, P.-J.; Hsu, C.-S. *Adv. Funct. Mater.* **2011**, *21*, 1723. (e) Klimov, E.; Li, W.; Yang, X.; Hoffmann, G. G.; Loos, J. *Macromolecules* **2006**, *39*, 4493. (f) Zhong, H.; Yang, X.; deWith, B.; Loos, J. *Macromolecules* **2006**, *39*, 218. (g) Muller, C.; Ferenczi, T. A. M.; Campoy-Quiles, M.; Frost, J. M.; Bradley, D. D. C.; Smith, P.; Stingelin-Stutzmann, N.; Nelson, J. *Adv. Mater.* **2008**, *20*, 3510.

(8) (a) Riedel, I.; von Hauff, E.; Parisi, J.; Martín, N.; Giacalone, F.; Dyakonov, V. *Adv. Funct. Mater.* **2005**, *15*, 1979. (b) Sánchez-Díaz, A.; Izquierdo, M.; Filippone, S.; Martin, N.; Palomares, E. *Adv. Funct. Mater.* **2010**, *20*, 2695. (c) Bolink, H. J.; Coronado, E.; Forment-Aliaga, A.; Lenes, M.; La Rosa, A.; Filippone, S.; Martin, N. *J. Mater. Chem.* **2011**, *21*, 1382. (d) Garcia-Belmonte, G.; Boix, P. P.; Bisquert, J.; Lenes, M.; Bolink, H. J.; La Rosa, A.; Filippone, S.; Martín, N. *J. Phys. Chem. Lett.* **2010**, *1*, 2566.

(9) Eiermann, M.; Haddon, R. C.; Knight, B.; Li, Q. C.; Maggini, M.; Martín, N.; Ohno, T.; Prato, M.; Suzuki, T.; Wudl, F. *Angew. Chem., Int. Ed.* **1995**, *34*, 1591.

(10) Roy, S.; Nangia, A. *Cryst. Growth Des.* **2007**, *7*, 2047.

(11) Yang, D. Y.; Han, O.; Liu, H. W. *J. Org. Chem.* **1989**, *54*, 5402.